

# Physics cross section and events generation on CEPC\*

Xin. Mo<sup>1,2;1)</sup> Gang. Li<sup>1,2;1)</sup><sup>1</sup> Institute of High Energy Physics, Chinese Academy of Sciences, Beijing 100049, China

**Abstract:** The cross sections of Higgs signal and background production at CEPC are calculated by the Monte-Carlo method, and the beam-strahlung effect due to accelerator is carefully investigated. The classification of event samples for CEPC is discussed. The potential new physics beyond the Standard Model Higgs is discussed as well.

**Key words:** CEPC, cross section, Monte-Carlo generation

## 1 Introduction

The discovery of Higgs boson [1, 2] is a great milestone for the modern particle physics. No matter whether it is just the Standard Model (SM) Higgs or an indication of anything else in new physics, the fact that it is found in the search of SM Higgs boson makes the Higgs mechanism more creditable. Furthermore, precision measurements of properties for the new Higgs-like boson are the critical points in the Higgs physics, any deviation from the SM expectation will improve our knowledge of the fundamental particles and their interaction. With this consideration, machine with high luminosity and an ideal environment is much more appropriate in Higgs research.

The Circular Electron-Positron Collider(CEPC) [3] is a proposed circular electron positron collider for next generation. It is designed to run around 240~250 GeV and deliver 5 ab<sup>-1</sup> of integrated luminosity for 10 years totally. About 10<sup>6</sup> Higgs events will be produced, and this large statistic and clean environment enable CEPC to measure the cross section of Higgs production as well as its mass, decay width and branching ratios with precision far beyond the hadron colliders.

Besides the Higgs events, there will be a large number of electroweak processes generated at the same time, via the electroweak vector bosons W and Z. The electroweak events also play an important role in the  $e^+e^-$  colliders. On one hand, these events are the major backgrounds of the Higgs precision measurements; on the other hand, they are useful to calibrate the detector precisely for the following measurements of Higgs boson properties.

The calculation in this work is done by WHIZARD [5, 6], which is one of the most popular Monte-Carlo generators for the Higgs study and is employed by ILC and

CLIC group as well.

In this paper, we will investigate the physics cross sections and discuss the events generation work on the CEPC. In Sec. II the Higgs production is investigated and the cross sections are given. The radiative correction of cross sections will be discussed in Sec. III. In Sec. IV, the backgrounds with various final states is the main topic of this section. Finally, a brief summary will be given in the Sec. V.

## 2 Higgs production cross section

Due to the fact that the Higgs boson coupling to fermions is proportional to the fermion mass, the dominant Higgs production in electron positron annihilation is the so-called Higgsstrahlung, a  $s$ -channel process in which Higgs is produced in association with a Z boson, as shown in Fig. 7.

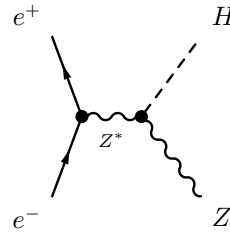


Fig. 1. The Feynman diagrams of the Higgsstrahlung process

The other two typical  $t$ -channel processes, called as vector boson fusion, will become more significant and give a sizable contribution to the Higgs production along with the increase of center of mass energy, .

\* The study was partially supported by the CAS/SAFEA International Partnership Program for Creative Research Teams and funding from CAS and IHEP for the Thousand Talent and Hundred Talent programs, as well as grants from the State Key Laboratory of Nuclear Electronics and Particle Detectors.

1) E-mail: moxin@ihep.ac.cn

2) E-mail: li.gang@ihep.ac.cn

©2013 Chinese Physical Society and the Institute of High Energy Physics of the Chinese Academy of Sciences and the Institute of Modern Physics of the Chinese Academy of Sciences and IOP Publishing Ltd

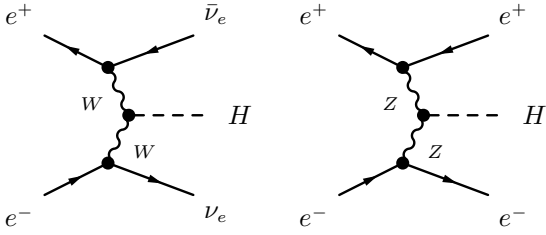


Fig. 2. The Feynman diagrams of vector boson fusion

The cross section of the Higgsstrahlung can be written as

$$\sigma(e^+e^- \rightarrow ZH) = \frac{G_F^2 m_Z^4}{96\pi s} (v_e^2 + a_e^2) \lambda^{\frac{1}{2}} \frac{\lambda + 12m_Z^2/s}{(1 - m_Z^2/s)^2}. \quad (1)$$

And the cross section for the vector fusion production can be written in a similar compact form as [7]

$$\sigma(e^+e^- \rightarrow VV \rightarrow l\bar{l}H) = \frac{G_F^3 m_V^4}{4\sqrt{2}\pi^3} \int_{x_H}^1 dx \int_x^1 \frac{dy F(x,y)}{[1 + (y-x)/x_V^2]^2}, \quad (2)$$

$$F(x,y) = \left( \frac{2x}{y^3} - \frac{3x+1}{y^2} + \frac{x+2}{y} - 1 \right) \left[ \frac{z}{z+1} - \log(z+1) \right] + \frac{xz^2(1-y)}{y^3(z+1)},$$

where V stands for vector bosons Z and W, respectively, and the dimensionless variables are defined as

$$x_H = m_H^2/s, \quad x_V = m_V^2/s \quad z = y(x - x_H)/(xx_V).$$

For the moderate Higgs masses and energies, the cross section of vector boson fusion is suppressed compared with the Higgsstrahlung due to the additional electroweak couplings. With the increasing energy, the cross section of fusion process rises in a logarithmic manner as the expected typical  $t$ -channel process [8]

$$\sigma(e^+e^- \rightarrow VV \rightarrow l\bar{l}H) \approx \frac{G_F^3 m_V^4}{4\sqrt{2}\pi^3} \log \frac{s}{m_H^2}, \quad (3)$$

therefore it will become the dominant contribution to the Higgs production. Meanwhile, the cross section of the Higgsstrahlung decreases according to the scaling law  $\sim g_F^4/s$  asymptotically.

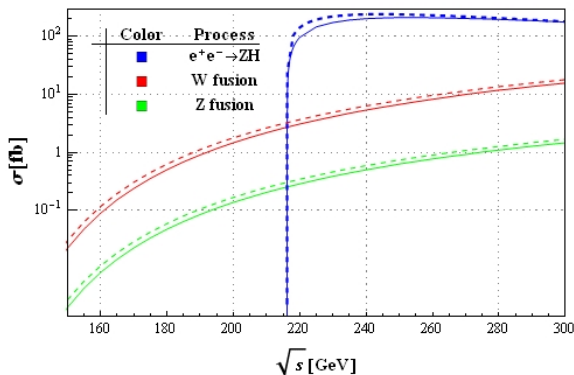


Fig. 3. The cross sections of various Higgs production

The behavior of Higgsstrahlung,  $WW$  fusion and  $ZZ$  fusion is shown in Fig.3. Above the threshold of  $ZH$ , the cross section of Higgsstrahlung rises rapidly and reaches its maximum around 240 ~ 250 GeV. The dashed line represent the cross sections without ISR effect which will be discussed in the following section.

### 3 Radiative correction

The Initial State Radiation (ISR) is an important issue in high energy processes, in particular to lepton collider. It is in fact the largest higher order correction for the fundamental QED processes. Though the cancellation for soft and collinear photons has been validated to all orders in perturbation theory [9], and the hard photon emission could also be calculated perturbatively order by order in QED [10, 11]. Actually, the maximal order for the hard photon is set to be 3 in the calculation.

Besides ISR, another macro effect at high luminosity electron-positron collider, beamstrahlung, also affects the cross section. In the storage ring the beamstrahlung effect makes the beam energy spread larger and the center of mass energy smaller. The popular tool used to simulate this effect for  $e^+e^-$  colliders is GuineaPig++ [12, 13]. Based on the simulation the energy spread due to beamstrahlung is determined and the total energy spread caused by beamstrahlung and synchrotron radiation is 0.1629 at CEPC% [4]. With both the beam spread and beamstrahlung taken into account during the calculation, it is proved that the correction on the Higgs cross section due to this effect is negligible, the comparison results are listed in Tab.1.

Table 1. Comparison of cross sections for beamstrahlung on and off

	ISR	ISR & beamstrahlung
$\sigma(e^+e^- \rightarrow f\bar{f}H)$ [fb]	208.87	208.67

## 4 Cross sections of backgrounds

### 4.1 Two fermions backgrounds

Those events with two fermions in final states are one of the major backgrounds in electron positron collider. The leading process is the quark pair production since its cross section is 50 pb at 240 GeV. Another notable two fermions process is the di-muon production, whose cross section reaches 5 pb.

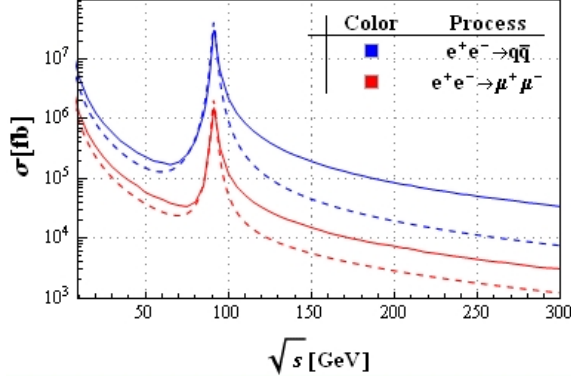


Fig. 4. The cross sections of various Higgs production

The cross sections are much higher in the vicinity of Z pole and the improvements for the precision of Z pole measurement could benefit from such a large statistic.

Table 2. The proposed scan around Z pole on CEPC

$\sqrt{s}$ [GeV]	88.2	89.2	90.2	91.1876	92.2	93.2	94.2
$L$ [fb $^{-1}$ ]	10	10	10	100	10	10	10
$\sigma(e^+e^- \rightarrow q\bar{q})$ [nb]	4.22	7.92	17.22	30.20	22.24	12.78	8.18
$\sigma(e^+e^- \rightarrow \mu\mu)$ [nb]	0.22	0.41	0.87	1.51	1.11	0.65	0.42

## 4.2 Bhabha scattering

The small-angle(SABH) and larger-angle(LABH) Bhabha scattering events both play roles in  $e^+e^-$  collider physics. SABH is mainly used to measure the instant luminosity of the accelerator due to the huge cross section, while LABH can be used as cross check of the luminosity measurement of the SABH and the calibration of detector.

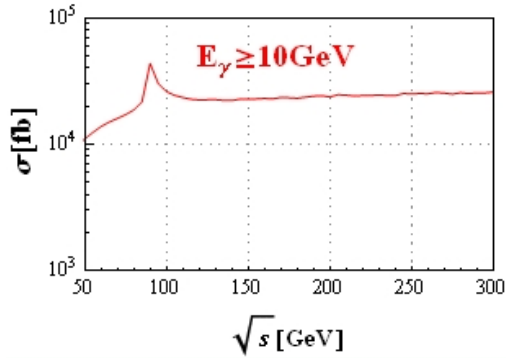


Fig. 5. The cross sections of Bhabha process, ISR is included and a cut for photon energy is applied.

The cross section of SABH in next-to-leading order for theoretical prediction depends not only on the angular range covered by detector, but also on the cut of the electron energy. Although the WHIZARD is designed to

calculate it up to next leading order, unfortunately, it is not an proper tool for SABH process. For LABH, the Bhabha process actually become to be the radiative Bhabha  $e^+e^- \rightarrow e^+e^-\gamma$ . If the energy of the emitted photon is large enough compared with the detection threshold, the event can be recorded and the contribution of this kind of background can be estimated by the corresponding cross section. In WHIZARD, this cross section is calculated by setting a cut.

Due to the cut applied, the peak at Z pole is not as sharp as  $q\bar{q}$  or  $\mu^+\mu^-$ , but the value at 240GeV still reaches much higher and will contribute much more.

## 4.3 Vector boson pair production

The electroweak processes for vector boson pair production are  $e^+e^- \rightarrow W^+W^-$  and  $e^+e^- \rightarrow ZZ$ . The cross section of on-shell production for vector bosons is plotted in Fig.6. The s-channel process provides the dominant contribution in the CEPC energy region.

Kinematically, W bosons can decay into a quark-antiquark pair, for example  $W^+W^- \rightarrow u\bar{u}d\bar{d}$  or  $c\bar{c}s\bar{s}$ , creating four jets similar to the Higgs boson signal. Although ZZ pair production is one magnitude smaller than WW, it is especially severe for the background of the Higgs measurements as it may lead to the same final states as ZH production and the kinematic is very similar with ZH.

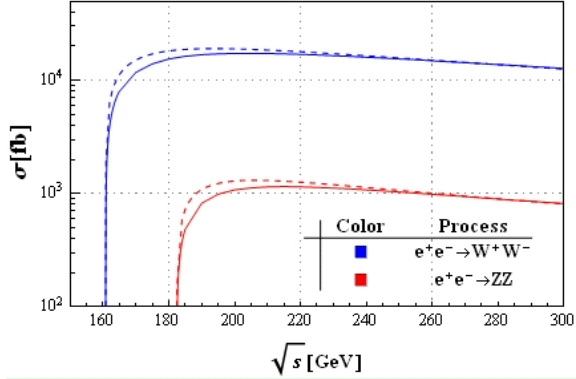


Fig. 6. The cross sections of various Higgs production

The precision measurements for W boson mass can be achieved by the direct measurement method. By applying the direct method, no additional energy scans are needed, the measurements can be performed with the same run at  $\sqrt{s} = 240\text{GeV}$  where most attention is paid on Higgs. The main challenge of direct method is calibration of the measured momentum and energy and the resolution effect, which is proportional to  $\sqrt{s}$ . Thanks to the high luminosity of CEPC, the uncertainty due to the beamstrahlung can be reduced to the 1MeV.

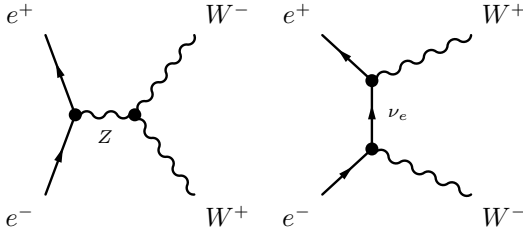


Fig. 7. The Feynman diagrams of WW pair production

Besides the W boson mass measurements, these vector boson productions are also a good resource for the precision measurements for triple boson coupling of electroweak theory. Any deviation from SM caused by the virtual new particles will be the hint of new physics beyond the standard model.

For the process  $e^+e^- \rightarrow ZZ$ , it is not as attractive as the  $e^+e^- \rightarrow W^+W^-$ . The study for  $e^+e^- \rightarrow ZZ$  mainly serves as data-driven background in Higgs analysis via sideband.

## 5 Classification of event samples

The Monte-Carlo event samples generated for CEPC could be classified into signal part and background part intuitively. The signal part includes all the Higgs production processes, both Higgsstrahlung and fusion. The backgrounds could be classified according to the final states furthermore. The final states with two fermions and four fermions contributes most the backgrounds for

CEPC, since the CEPC running energy region is not high enough for more particles in final state.

The classification for four fermions production depends on crucially on the final state, the schedule could be borrowed from LEP [18]. The four fermions can be classified into two classes, the first one comprises the (up, anti-down) and (down anti-up) quark pairs,

$$(U_i \bar{D}_i) + (\bar{U}_j D_j),$$

which is produced by virtual WW pair, named as “WW” process. The other class is the production of two fermion-antifermion pairs,

$$(f_i \bar{f}_i) + (\bar{f}_j f_j),$$

which is produced by two virtual neutron vector bosons, named as “ZZ” process.

Table 3. Number of Feynman diagrams for WW type processes

	$u\bar{d}$	$c\bar{s}$	$\bar{e}\nu_e$	$\bar{\mu}\nu_\mu$	$\bar{\tau}\nu_\tau$
$d\bar{u}$	43	11	20	10	10
$s\bar{c}$	11	44	20	10	10
$e\bar{\nu}_e$	20	20	56	18	18
$\mu\bar{\nu}_\mu$	10	10	18	19	9
$\tau\bar{\nu}_\tau$	10	10	18	9	20

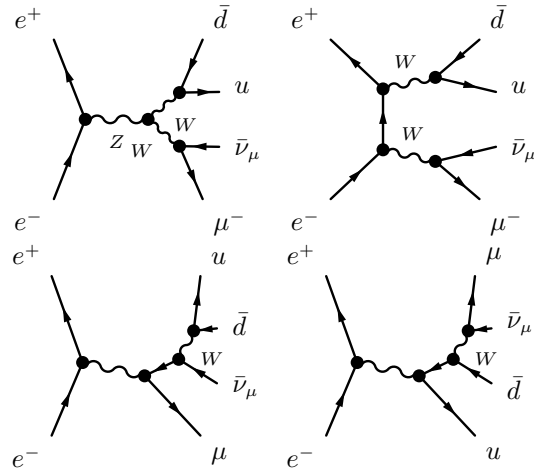


Fig. 8. The typical structure of four fermions production via two W bosons

A further restriction can be applied to these two types. If there are  $e^\pm$  together with its neutrino in the final state, and left a W boson on-shell, this type is named as “Single W” process; Meanwhile, if there are a electron-positron pair in the final state and a Z boson left on-shell, the case is named as “Single Z”. Some final states consists of two mutually charge conjugated fermion pairs, which could be from both virtual WW or ZZ, this type is called as “mixed type”.

The typical structure of Feynman diagrams for WW type is listed in Fig.8, the final states could be produced through double W pole or W boson radiation. Further, the actual number of the Feynman diagrams is listed in Tab.3. The number in **bold** font is the general WW process, which means the there are two pairs in final state without identical particles. The ordinary font and *italic* font describe the single W and mixed processes respectively. The ZZ type has a similar structure with the WW type, and Ref. [18] is a good reference for details.

## 6 Summary

As a summary, the cross sections of major processes for standard model, including Higgs production as well as the critical backgrounds are plotted in Fig.9, in which the ISR effect has been taken into account.

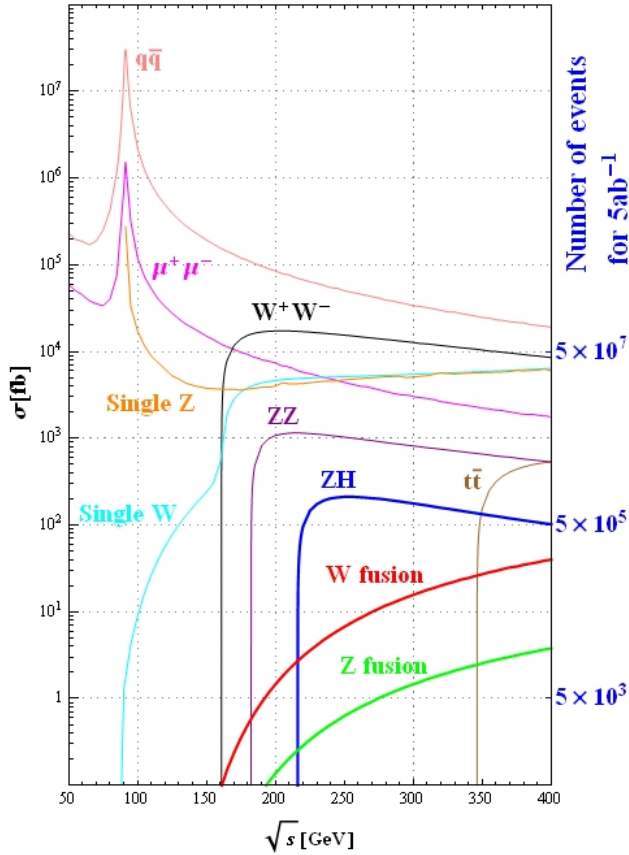


Fig. 9. The cross sections of major processes of SM with ISR effect taken into account.

Also the numerical value of these processes are listed in Tab.4, as well as the expected number of events for a 10-years running in  $5 \text{ ab}^{-1}$  luminosity total. According to the cross sections, the Monte-Carlo samples for Higgs analysis on CEPC have been generated by WHIZARD.

Table 4. The cross sections and number of events expected at 250 GeV

Process	Cross section	No. of events in $5\text{ab}^{-1}$
Higgs production cross section in fb		
$e^+e^- \rightarrow ZH$	212	$1.06 \times 10^6$
$e^+e^- \rightarrow \nu\bar{\nu}H$	6.27	$3.36 \times 10^4$
$e^+e^- \rightarrow e^+e^-H$	0.63	$3.15 \times 10^3$
Total	219	$1.10 \times 10^6$
Background processes cross section in pb		
$e^+e^- \rightarrow e^+e^-$	25.1	$1.3 \times 10^8$
$e^+e^- \rightarrow qq$	50.2	$2.5 \times 10^8$
$e^+e^- \rightarrow \mu\mu(\text{or}\tau\tau)$	4.40	$2.2 \times 10^7$
$e^+e^- \rightarrow WW$	15.4	$7.7 \times 10^7$
$e^+e^- \rightarrow ZZ$	1.03	$5.2 \times 10^6$
$e^+e^- \rightarrow eeZ$	4.73	$2.4 \times 10^7$
$e^+e^- \rightarrow e\nu W$	5.14	$2.6 \times 10^7$

In this paper, the cross sections of Higgs production and its background processes at the CEPC are evaluated and the classification for the MC samples is discussed. Most of the processes are well calculated by WHIZARD. Besides that, Bhabha process should be studied more carefully by some other specialized tools.

## References

- ATLAS Collaboration, G. Aad et al., Phys. Lett. B, 2012, **716**: 1–29
- CMS Collaboration, S. Chatrchyan et al., Phys. Lett. B, 2012, **716**: 30–61,
- CEPC-SppC Preliminary Conceptual Design Report: Physics and Detector, by the CEPC Study Group, to be released.
- CEPC Accelerator Preliminary Conceptual Design Report, by the CEPC Study Group, to be released.
- W. Kilian, T. Ohl, J. Reuter, Eur. Phys. J. C, 2011, **71**:1742.
- M. Moretti, T. Ohl, J. Reuter, arXiv: hep-ph/0102195.
- Proceedings of the Workshop  $e^+e^-$  Collisions at 500 GeV: The Physics Potential, Munich-Annecy-Hamburg, ed. P.M. Zerwas, Reports DESY 92-123A,B; 93-123C.
- W. Kilian, M. Kramer and P. M. Zerwas, Phys. Lett. B, 1996, **373**:135-140.
- V. N. Gribov and L. N. Lipatov, Sov. J. Nucl. Phys, 1972, **15**:675.
- E. A. Kuraev and V. S. Fadin, Sov. J. Nucl. Phys, 1985, **41**:466.
- M. Skrzypek and S. Jadach, Z. Phys. C, 1991, **49**:577.
- D. Schulte, CERN-PS-99-014-LP.
- D. Schulte, M. Alabau, P. Bambade, O. Dadoun, G. Le Meur, C. Rimbault and F. Touze, Conf. Proc. C, 2007, **070625**:2728.
- ALEPH Collaboration Collaboration, A. Heister et al., Eur. Phys. J. C, 2001, **22**:201C215.
- OPAL Collaboration Collaboration, G. Abbiendi et al., Phys. Lett. B, 2002, **546**:29C47.
- DELPHI Collaboration Collaboration, J. Abdallah et al., Eur. Phys. J. C, 2005, **40**:1C25.
- L3 Collaboration Collaboration, M. Acciarri et al., Phys. Lett. B, 1999, **448**:152C162.
- D. Bardina, M. Bilenkya, D. Lehnerc, A. Olchevskib and T. Riemann, Nucl. Phys. Proc. Suppl. B, 1994, **37**:148-157.